Inorganic Chemistry
Article

Inorg. Chem. **2010**, *49*, 7663–7675 **7663**
DOI: 10.1021/ic902335z

Seleno-Auranofin (Et_3PAuSe-tagl): Synthesis, Spectroscopic (EXAFS, ^{197}Au Mössbauer, ^{31}P, ^{1}H, ^{13}C, and ^{77}Se NMR, ESI-MS) Characterization, Biological Activity, and Rapid Serum Albumin-Induced Triethylphosphine Oxide Generation

David T. Hill,*,‡ Anvarhusein A. Isab,§,∥ Don E. Griswold,⊥ Michael J. DiMartino,⊥ Elizabeth D. Matz,¶ Angel L. Figueroa,¶ Joyce E. Wawro,¶ Charles DeBrosse,‡ William M. Reiff,# Richard C. Elder,††,▽ Benjamin Jones,▽ James W. Webb,† and C. Frank Shaw III*,†,§

†*Department of Chemistry, Illinois State University, Normal Illinois 61790-4160,* ‡*Department of Chemistry, Temple University, Philadelphia, Pennsylvania 19122,* §*Department of Chemistry, University of Wisconsin−Milwaukee, Milwaukee, Wisconsin 53201,* ∥*Department of Chemistry, King Fahd University of Petroleum and Minerals, Dhahran 31261, Saudi Arabia,* ⊥*Departments of Pharmacology, and* ¶*Analytical Chemistry, GlaxoSmithKline Pharmaceuticals, 709 Swedeland Road, King of Prussia, Pennsylvania 19406-0939,* #*Department of Chemistry, Northeastern University, Boston, Massachusetts 02115, and* ▽*Department of Chemistry, University of Cincinnati, Cincinnati Ohio 45221-0172.* ††*Deceased.*

Received November 25, 2009

Seleno-auranofin (SeAF), an analogue of auranofin (AF), the orally active antiarthritic gold drug in clinical use, was synthesized and has been characterized by an array of physical techniques and biological assays. The Mössbauer and extended X-ray absorption fine structure (EXAFS) parameters of the solid compound demonstrate a linear P−Au−Se coordination environment at a gold(I) center, analogous to the structure of auranofin. The ^{31}P, ^{13}C, and ^{1}H NMR spectra of SeAF in chloroform solution closely resemble those of auranofin. The ^{77}Se spectrum consists of a singlet at 481 ppm, consistent with a metal-bound selenolate ligand. The absence of $^{2}J_{PSe}$ coupling in the ^{31}P and ^{77}Se spectra may arise from dynamic processes occurring in solution or because the $^{2}J_{PSe}$ coupling constants are smaller than the observed bandwidths. Electrospray ionization mass spectrometry (ESI-MS) spectra of SeAF in 50:50 methanol−water exhibited strong signals for $[(Et_3P)_2Au]^+$, $[(Et_3PAu)_2$-μ-Se-tagl$]^+$, and $[Au(Se\text{-}tagl)_2]^-$, which arise from ligand scrambling reactions. Three assays of the anti-inflammatory activity of SeAF allowed comparison to AF. SeAF exhibited comparable activity in the topically administered murine arachadonic acid-induced and phorbol ester-induced anti-inflammatory assays but was inactive in the orally administered carragenan-induced assay in rats. However, in vivo serum gold levels were comparable in the rat, suggesting that differences between the in vivo metabolism of the two compounds, leading to differences in transport to the inflamed site, may account for the differential activity in the carrageenan-induced assay. Reactions of serum albumin, the principal transport protein of gold in the serum, demonstrated formation of $AlbSAuPEt_3$ at cysteine 34 and provided evidence for facile reduction of disulfide bonds at cysteine 34 and very rapid formation of $Et_3P{=}O$, a known metabolite of auranofin.

Introduction

Auranofin (**1**) (AF, Et_3PAuS-tagl), a triethylphosphine-coordinated gold(I) thioglucose, first described in 1972,[1] has been used clinically for over three decades in the treatment of rheumatoid arthritis (RA).[2] Because of its immunopharmacological properties,[3] AF (**1**) has also been clinically evaluated for the treatment of juvenile arthritis,[4] psoriasis,[5] and steroid-dependent asthma.[6] In the latter disease, certain chrysotherapeutic agents, such as the oligomeric thiolates, gold thioglucose, and gold sodium thiomalate, which are administered by injection,

*Corresponding authors. E-mail: cfshaw@ilstu.edu (C.F.S) and hill@temple.edu (D.T.H).

(1) Sutton, B. M.; McGusty, E.; Walz, D. T.; DiMartino, M. J. *J. Med. Chem.* **1972**, *15*, 1095–1098.

(2) (a) Finkelstein, A. E.; Walz, D. T.; Batista, V.; Misraji, M.; Roisman, F.; Misher, A. *Ann. Rheum. Dis.* **1976**, *35*, 251–257. (b) Glennas, A.; Kvien, T. K.; Andrup, O.; Clarke-Jenssen, O.; Karstensen, B.; Brodin, U. *Br. J. Rheumatol.* **1997**, *36*, 870–877. (c) Hamada, Y.; Shinomiya, F; Okada, M.; Fujimura, T. *Mod. Rheumatol.* **2003**, *13*, 27–34.

(3) (a) Lewis, A. J.; Walz, D. T. *Prog. Med. Chem.* **1982**, *19*, 1–58. (b) Walz, D. T.; Griswold, D. E. *Inflammation* **1978**, *3*, 117–28.

(4) (a) Brewer, E. J., Jr.; Giannini, E. H.; Person, D. A. *Am. J. Med.* **1983**, *75*, 152–156. (b) Giannini, E. H.; Barron, K. S.; Spencer, C. H.; Person, D. A.; Baum, J.; Bernstein, B. H.; Kredich, D. W.; Jacobs, J. C.; Zemel, L. S.; Gibbas, D. *J. Rheumatol.* **1991**, *18*, 1240–2.

(5) Helm, K. F.; Marks, J. G., Jr.; Leyden, J. J.; Krueger, G. G.; Griffiths, T. W.; Griffiths, C. E. *J. Am. Acad. Dermatol.* **1995**, *33*, 517–519.

(6) Bernstein, I. L.; Bernstein, D. I.; Dubb, J. W.; Faiferman, I.; Wallin, B.; Bronsky, E.; Spector, S. L.; Nathan, R. A.; Nelson, H. S.; et al. *J. Allergy Clin. Immunol.* **1996**, *98*, 317–324.

Published on Web 08/12/2010

have had a long tradition of use, particularly in Japan.[7] AF (**1**), on the other hand, is effective when given orally, both in the treatment of RA and psoriatic arthritis.[8] The biological mechanism of action of gold-based drugs remains undeciphered in its totality. However, its behavior in biological systems has been the object of intense study,[9] and significant progress has been made. A key aspect of the biochemical behavior of gold agents is the displacement of a coordinating sulfur ligand by naturally occurring sulfhydryl compounds.[10−14] In the exchange reaction with albumin, the tetraacetylthioglucose portion of AF is displaced by the SH of cysteine-34,[11,13] the only reduced cysteine residue, to form AlbSAuPEt$_3$.[11−14] This is followed by displacement of the phosphine ligand and the generation of Et$_3$PO.[11−14] The rate of in vitro generation of Et$_3$PO from AlbSAuPEt$_3$ is fastest for the thiolate ligands that have the greatest affinity for gold.[11] AF also reacts in vivo and in whole blood to form Et$_3$PO as a metabolic product.[12] Studies of related AF analogues suggest that for R$_3$PAuX, increasing the bulk and basicity of the phosphine (R = CH_3 < CH_3CH_2 < $(CH_3)_2CH$) retards its oxidation to R$_3$P═O. Conversely increasing the affinity of the anion for gold(I) favors oxidation and formation of phosphine oxide.[11]

Since selenols have higher affinities for mercury(II) and gold(I) than do thiols and also undergo more rapid exchange with disulfides than do thiols,[15] it was of interest to us to prepare seleno-auranofin (**2**) (SeAF, Et$_3$PAuSe-tagl) and to compare its biological and bioinorganic behavior with AF. In addition, we sought further insight into the chemistry of cysteine-34 of albumin in the reduced (thiolate) and oxidized (disulfide with a nonprotein thiol) states with gold compounds.

The reactions of auranofin and other gold(I) species with selenoproteins are significant for their metabolism and enzymology[16−19] and in the development of treatments for arthritis,[9d,20,21] cancer,[9e,21−24] and a variety of parasitic[25−28] and infectious[29] diseases. Numerous gold(I) model complexes with selenium ligands have been characterized,[30−36] and the field has recently been reviewed.[37]

Described herein is the synthesis and spectroscopic characterization (EXAFS, ^{197}Au Mössbauer, and ^{1}H, ^{13}C, ^{31}P, ^{77}Se NMR, and ESI-MS) of SeAF. The results of in vitro ligand exchange studies with albumin and cysteine-modified albumin using ^{31}P NMR spectroscopy and chromatographic separation are reported. SeAF was tested in vivo against three immunological models related to inflammation and RA. Only one report[38] and two patents[39,40] describing the synthesis of SeAF have appeared in the literature, but no information regarding its solution chemistry, biochemistry, or biological activity has been presented subsequently.

Experimental Methods

Materials. Sephadex G-50 and 5,5′-dithiobis(2-nitrobenzoic acid) were obtained from Sigma Biochemicals; BSA (fatty acid free, lot no. 10740823−51) from Boehringer Mannheim Biochemicals Co.; and Iodoacetamide-blocked BSA (Ac-BSA) was prepared as described previously.[11] Cysteine-blocked BSA (Cys-BSA lot no. 11 m) from Miles Chemical Co.; D_2O (99.8 d),

(7) (a) Miyamoto, T.; Miyaji, S.; Horiuchi, Y.; Hara, M.; Ishihara, K. *J. Jpn. Soc. Int. Med.* **1974**, *63*, 1190–1197. (b) Yoshizawa, H.; Azuma, T.; Hazama, T. *Ryumachi* **1973**, *13*, 366–7. (c) Oka, Y. *Ryumachi* **1973**, *12*, 311–23.
(8) Bernstein, D. I.; Bernstein, I. L.; Bodenheimer, S. S.; Pietrusko, R. G. *J. Allergy Clin. Immunol.* **1988**, *81*, 6–16.
(9) (a) *Proceedings of the Symposium on Bioinorganic Chemistry of Gold Coordination Compounds*; Sutton, B. M., Franz, R. G., Eds.; Smith Kline and French Laboratories: Philadelphia, PA, 1981. (b) Shaw, C. F. III. *The Biochemistry of Gold*; Schmidbaur, H., Ed.; John Wiley & Sons: Chichester, U.K., 1999; pp 250−308. (c) Shaw, C. F., III. *Chem. Rev.* **1999**, *99*, 2589–2600. (d) Messori, L.; Marcon, G. *Met. Ions Biol. Syst.* **2004**, *41*, 279–304. (e) Messori, L.; Marcon, G. *Met. Ions Biol. Syst.* **2004**, *42*, 385–425.
(10) (a) Shaw, C. F., III.; Schaeffer, N. A.; Elder, R. C.; Eidsness, M. K.; Trooster, J. M.; Calis, H. M. G. *J. Am. Chem. Soc.* **1984**, *106*, 3511–3521. (b) Isab, A. A.; Hormann, A. L.; Hill, D. T.; Griswold, D. E.; Martino, M. J.; Shaw, C. F., III. *Inorg. Chem.* **1989**, *28*, 1321–1326.
(11) (a) Coffer, M. T.; Shaw, C. F., III.; Hormann, A. L.; Mirabelli, C. T.; Crooke, S. T. *J. Inorg. Biochem.* **1987**, *30*, 177–187. (b) Isab, A. A.; Shaw, C. F., III.; Locke, J. *Inorg. Chem.* **1988**, *27*, 3406–3409.
(12) Intoccia, A. P.; Flanagan, T. L.; Walz, D. T.; Gutzait, L.; Swagzdis, J. E.; Flagiello, J. Jr.; Hwang, B.Y-H.; Dewey, R. H. In *Proceedings of the Symposium on Bioinorganic Chemistry of Gold Coordination Compounds*; Smith Kline and French Laboratories: Philadelphia, PA, 1981, pp21−33.
(13) (a) Malik, N. A.; Otiko, G.; Razi, M. T.; Sadler, P. J. *J. Inorg. / Biochem.* **1980**, *12*, 317–322. (b) Malik, N. A.; Otiko, G.; Razi, M. T.; Sadler, P. J. in Sutton, B. M.; Franz, R. G., Eds., Proceedings of the Symposium on Bioinorganic Chemistry of Gold Coordination Compounds, Smith Kline and French Laboratories; Philadelphia, PA, 1981, pp 82−97.
(14) Coffer, M. T.; Shaw, C. F., III.; Eidness, M. K.; Watkins, J. W., II.; Elder, R. C. *Inorg. Chem.* **1986**, *25*, 333–340.
(15) (a) Arnold, A. P.; Tan, K. S.; Rabenstein, D. L. *Inorg. Chem.* **1986**, *25*, 2433–2437. (b) Isab, A. A. *Transition Met. Chem.* **1994**, *19*, 495–498. (c) Pleasants, J. C.; Guo, W.; Rabenstein, D. L. *J. Am. Chem. Soc.* **1989**, *111*, 6553–6558. (d) Lewis, S. D.; Misra, D. C.; Shafer, J. A. *Biochemistry* **1980**, *19*, 6129–6137.
(16) Becker, K.; Gromer, S.; Schirmer, R. H.; Müller, S. *Eur. J. Biochem.* **2000**, *267*, 6118–6125.
(17) Gromer, S.; Arscott, L. D.; Williams, C. H., Jr.; Schirmer, R. H. *J. Biol. Chem.* **1998**, *32*, 20096–20101.
(18) Steinbrenner, H.; Bilgic, E; Alili, L.; Sies, H.; Brenneisen, P.. *Free Radical Res.* **2006**, *40*, 936–943.
(19) Lothrop, A. P.; Ruggles, E. L.; Honda, R. J. *Biochemistry* **2009**, *48*, 6213–6223.
(20) Roberts, J. R.; Shaw, C. F., III. *Biochem. Pharmacol.* **1998**, *55*, 1291–1299.
(21) Ott, I. *Coord. Chem. Rev.* **2010**, *253*, 1670–1681.
(22) Hickey, J. L.; Ruhayel, R. A.; Barnard, P. J.; Baker, M. V.; Berners-Price, S. J.; Filipovska, A. *J. Am. Chem. Soc.* **2008**, *130*, 12570–12571.
(23) Talbot, S.; Nelson, R.; Self, W. T. *Br. J. Pharmacol.* **2008**, *154*, 940–948.
(24) Rigobello, M. P.; Gandin, V.; Folda, A.; Rundlöf, A. K.; Fernandes, A. P.; Bindoli, A.; Marzano, C.; Björnstedt, M. *Free Radical Biol. Med.* **2009**, *47*, 710–721.
(25) Bonilla, M.; Denicola, A.; Novoselov, S. V.; Turanov, A. A.; Protasio, A.; Izmendi, D.; Gladyshev, V. N.; Salinas, G. *J. Biol. Chem.* **2008**, *283*, 17898–17907.
(26) Kuntz, A. N.; Davioud-Charvet, E.; Sayed, A. A.; Califf, L. L.; Arnér, Williams, D. L. *PLoS Medicine* **2007**, *4*, 1071–1086.
(27) Lobanov, A. V.; Gromer, S.; Salinas, G.; Gladyshev, V. N. *Nucl. Acid Res.* **2006**, *34*, 4012–4024.
(28) Angelucci, F.; Sayed A. A.; Williams, D. L.;, Boumis, G.; Brunori, M.; Dimastrogiovanni, D.; Miele, A. E.; Pauly, F.; Bellelli, A. *J. Biol. Chem.* **2009**, *284*, 28977-28985.
(29) Jackson-Rosario, S.; Cowart, D.; Myers, A.; Tarrien, R.; Levine, R. L.; Scott, R. A.; Self, W. T. *J. Biol. Inorg. Chem.* **2009**, *14*, 485–496. (b) Jackson-Rosario, S.; Self, W. T. *J. Bacteriol.* **2009**, *191*, 4035–4040.
(30) (a) Du Mont, W.-W.; Kubiniok, S.; Lange, L.; Pohl, S.; Sock, W.; Wagner, I. *Chem. Ber.* **1991**, *124*, 1315–1320. (b) Wagner, I.; du Mont, W.-W. *J. Organomet. Chem.* **1990**, *395*, C23–C25.
(31) Jones, P. G.; Thöne, C. *Chem. Ber.* **1991**, *124*, 2725–2729.
(32) Ahmad, S.; Isab, A. A.; Al-Arfaj, A. R.; Arnold, A. P. *Polyhedron* **2002**, *21*, 2099–2105.
(33) Ahmad, S.; Isab, A. A.; Persanowski, H. P.; Hussain, M. S.; Akhtar, M. N. *Trans. Metal Chem.* **2002**, *27*, 177–183.
(34) Ahmad, S.; Akhtar, M. N.; Isab, A. A.; Al-Afraj, A. R.; Hussain, M. S. *J. Coord. Chem.* **2000**, *51*, 225–234.
(35) Bhabak, K. P.; Mugesh, G. *Inorg. Chem.* **2009**, *48*, 2449–2455.
(36) Isab, A. A.; Aktar, M. N.; Al-Arfaj, A. R. *J. Chem. Soc., Dalton Trans.* **1995**, 1483–1487.
(37) Molter, A.; Nohr, F. *Coord. Chem. Rev.* **2010**, *254*, 19–45.
(38) Pill, T.; Breu, W.; Wagner, H.; Beck, W. *Chem. Ber.* **1991**, *124*, 713–717.
(39) Stockel, R. F.; Duma, P. E. alpha,omega-bis(diphenylphosphino)-hydrocarbon bis(thiosugar)gold and bis(selenosugar)gold derivatives. U.S. Patent 4,680,286, 1987.
(40) Hill, D. T.; Johnson, R. K. Use of selenium-containing compounds for negating the toxic effects of gold compounds used in the treatment of rheumatoid arthritis, and a novel selenium-containing gold compound and use thereof as an anti-rheumatoid arthritis medicine. EP 0189306, assigned to Snamprogetti SpA, 1986.

HS-tagl, and selenourea were purchased from Aldrich Chemical Co. and used directly as received. Et_3PAuCl,[1] AF,[1] Et_3PAuCN,[41] and acetobromoglucose[42] were prepared as described in the literature.

2-(2,3,4,6-Tetra-O-acetyl-β-D-glucopyranosyl)-2-selenopseudourea Hydrobromide. Acetobromoglucose (33.2 g, 0.08 mol) and selenourea (10.0 g, 0.08 mol) in acetone (150 mL) were refluxed under argon for 2 h (precipitate appeared). After cooling overnight, the resulting product was collected, washed with cold acetone, and dried in vacuo to give 26.4 g (61%) of selenopseudourea hydrobromide; Mp 196−197 °C dec (uncor, darkens at 185 °C; lit[43] Mp 187−189 °C). This material was used in the next reaction without further purification.

(l-Seleno-β-D-glucopyranose-2,3,4,6-tetraacetato-Se)(triethylphosphine)gold(I) (SeAF). A solution of potassium carbonate (1.40 g, 0.010 mol) in water (10 mL) was added with stirring to a mixture of the selenopseudourea hydrobromide (5.34 g, 0.010 mol) in water (30 mL) and was kept at 0 °C. After 30 min, a solution of Et_3PAuCl (3.50 g, 0.010 mol) in ethanol (10 mL)/methylene chloride (5 mL) was added and stirring continued for an additional 30 min. The mixture was poured into water (200 mL) and extracted with methylene chloride (3 × 50 mL). The combined extracts were dried ($MgSO_4$), filtered, and the solvent removed at reduced pressure to give 6.48 g of white solid (crude product). Chromatography on silica gel, eluting with chloroform, gave 3.72 g (51%) of product, SeAF. Treatment with anhydrous ethyl ether followed by crystallization from aqueous methanol gave an analytical sample; Mp 97−100 °C (lit[44] Mp 52 °C); $[\alpha]_D^{25} = -55.4°$ (1% in CH_3OH). Anal. calcd for $C_{20}H_{34}AuO_9PSe$: C, 33.12; H, 4.72; P, 4.27; Se 10.89. Found: C, 33.06; H, 4.70; P, 4.27; Se, 10.70. ^{1}H NMR ($CDCl_3$: 05.28 (m, 1H, H_1); δ 5.09−5.05 (m, 3H, H_2, H_3, H_4); 4.22 (dd, 1H, J = 5.1 Hz, 12.2 Hz); 4.08 (dd, 1H, dd, J = 2.4 Hz); 3.66 (m, 1H, H_5); 2.06, 2.04, 1.99, 1.96 (all S, 12H, CH_3CO); 1.85 (m, 6H, PCH_2); 1.21 (m, 9H, CH_3-). ^{13}C[^{1}H]NMR ($CDCl_3$): δ 170.66 (S, CO); 170.21 (S, CO); 169.49 (S, CO); 169.44 (S, CO); 77.23 (S, C1, or C2); 74.19 (S, C3, or C5); 73.93 (S, C3, or C5); 68.88 (S, C4); 62.70 (S, C6); 21.15 (S, CH_3); 20.72 (S, CH_3); 20.60 (S, CH_3); 20.55 (S, CH_3); (S, CH_3); 17.94 (d, PCH_2, J = 31.94 Hz); 8.77 (S, CH_3). ^{31}P{^{1}H}NMR ($CDCl_3$): δ 35.11. ^{77}Se{^{1}H}NMR ($CDCl_3$): δ 417.8.

Mössbauer Spectroscopy. The ^{197}Au Mössbauer spectrum of SeAF (Figure 1) was obtained for 100 mg of finely powdered crystals in a nylon holder of 12 mm diameter and maintained at 4.2 K throughout the data collection. The ^{197}Pt Mössbauer source was generated via neutron irradiation of highly isotopically enriched (>90% ^{196}Pt) platinum foils and was also maintained at 4.2 K. The holder was wrapped in aluminum foil. The instrumentation used was previously described[45] and is based primarily on an integrating counting technique[46] in conjunction with a thin Tl-doped NaI (crystal) detector. The recorded spectrum was fitted to a single quadrupole doublet.[47] The isomer shift was measured relative to metallic gold foil. The ^{197}Au Mössbauer parameters of AF were measured similarly and agreed with literature values.[48]

X-ray Absorption Spectroscopy (XAS). XAS data were measured in transmission mode at the Stanford Synchrotron Radiation Laboratory (3.0 GeV, = 50 mA). The data were collected on the wiggler side station IV-3 at the gold L_m edge, 11921.2 eV, out to 14 A^{-1} and at the selenium K edge, 12660.0 eV, out to 13.5 A^{-1}. The absorption edge energies were calibrated to the gold L_m edge energy using a 0.01 mm gold foil as an internal calibrant. All data were measured in the solid phase at ∼17 K using a flowing helium cryostat (Oxford Instrument CF1208).

NMR Spectra. All the NMR data (^{1}H, ^{13}C, ^{31}P, and ^{77}Se) reported in the characterization of SeAF were obtained using a Bruker WM 360 spectrometer operating at 297 K and employing $CDCl_3$ as a solvent. Thus, the ^{1}H chemical shifts were measured at 360 MHz relative to tetramethylsilane; the ^{13}C{^{1}H} spectra were obtained at 90.56 MHz using tetramethylsilane as internal standard; the ^{31}P{^{1}H} chemical shift was recorded at 145.8 MHz employing trimethylphosphate ($(CH_3O)_3PO$) in $CDCl_3$ as the external standard ($\delta\ 31_P$ = 2.00 upfield from 85% phosphoric acid); the ^{77}Se{^{1}H} spectra were recorded at 68.75 MHz using diphenyldiselenide in $CDCl_3$ as the external standard ($\delta\ 77_{Se}$ = 481 relative to dimethylselenium in $CDCl_3$) at 29° and 55 °C. Low-temperature ^{31}P{^{1}H} spectra were measured from 20 to −27 °C in $CDCl_3$ and from ambient to −73 °C in CD_3OD.

Electrospray ionization (ESI) Mass Spectrometry. ESI mass spectra were recorded in both positive and negative ion mode using a Hewlett-Packard (Agilent) LC-MS (Series 1100 LC-MSD) with 40 V fragmentation voltage; 3500 V capillary voltage; N_2 flow 10 L/min @ 25 psi; ionization temperature of 250 °C. Samples (10.0 μL of 5 or 10 mM SeAF in 50:50 methanol−water, MeOH:H_2O, mixture) were injected into the ESI chamber. The flow rate was set at 0.400 mL/min. The mobile-phase solvent was also 50:50 MeOH:H_2O. The solvent composition and spray parameters were fixed for the analyses. Using the auto sampler, the delay time between mixing and the first spectral accumulation was typically 3 min.

Biomimetic Albumin-Binding Studies. ^{31}P{^{1}H} NMR Measurements. Preliminary to the BSA-binding experiments, ^{31}P{^{1}H} NMR spectra were obtained on solutions in deuterated 100 mM NH_4HCO_3 buffer, pH of 7.9, using a Bruker WM 250 multinuclear NMR spectrometer operating at 101.3 MHz. The ^{31}P NMR chemical shifts were measured and are reported relative to trimethylphosphate, TMP, as an internal reference. Approximately 5000−10 000 scans were accumulated for each spectrum.

^{31}P NMR Titrations of BSA with SeAF. Successive aliquots (61, 55, and 100 μL) of SeAF (50 mM in MeOH) were added to 2950 μL of BSA (SH titer 0.56; 4.10 mM BSA in 100 mM N_4HCO_3 buffer; pH of 7.9). After each addition, the NMR was measured, and a 100 μL sample was withdrawn and chromatographed to allow analysis of the protein-bound gold.

SeAF/Et_3PAuCN/AF Comparison. Three BSA solutions (4.30 mM; SH titer 0.56; 2.0 mL) were prepared in 100 mM NH_4HCO_3 buffer under argon atmosphere. SeAF, Et_3PAuCN, or AF (50 mM in MeOH; 110 μL) were added to the BSA solutions. The ^{31}P NMR spectra were recorded within 1.5 h and after 24 h. After the second NMR measurement, each sample was chromatographed, and the SH titer was measured.

Comparisons of Ac-BSA and Cys-BSA Reactions with SeAF. Ac-BSA (1.89 mM; SH titer <0.01) was prepared in 1950 μL of 100 mM NH_4HCO_3 buffer. SeAF (75 μL of 50 mM solution in MeOH) was added, and ^{31}P NMR spectrum was measured. Cys-BSA (4.39 mM; SH titer <0.06) was prepared in 2375 μL of buffer, and 200 μL of 50 mM SeAF in MeOH was added to it. The ^{31}P NMR spectrum was measured, and 100 μL of sample was withdrawn for chromatographic analysis of Au bonding. Successive aliquots (50, 50, and 100 μL) of Et_3PAuCl (100 mM in MeOH) were added to the Cys-BSA/SeAF mixture; after each addition, 100 μL of sample was withdrawn for analysis of gold-binding to albumin (vide infra). Two aliquots of tagl-SH (100 μL; 100 mM in MeOH) were added successively to the final Cys-BSA/SeAF/Et_3PAuCl reaction mixture. ^{31}P NMR spectra were accumulated after each addition.

Chromatographic Analysis of Gold Binding to BSA and Cys-BSA. Solutions of BSA (4.3 mM; SH titer 0.56) and Cys-BSA

(41) (a) Hormann, A. L.; Shaw, C. F., III.; Bennett, D. W.; Reiff, W. M. *Inorg. Chem.* **1986**, *25*, 3953–3957. (b) Hormann, A. L. Ph.D. Thesis, Unversity of Wisconsin, Milwaukee, 1988.
(42) Lemieux, R. U. *Methods Carbohydr. Chem.* **1963**, *2*, 221–222.
(43) Wagner, G.; Nuhn, P. *Ann. Pharm.* **1964**, *297*, 461–473.
(44) A Mp of 52 °C for SeAF is reported in reference 38; no Mp is disclosed in reference 39.
(45) Viegers, M. P. A.; Trooster, J. M. *Phys. Rev. B: Solid State* **1977**, *15*, 72–83.
(46) Viegers, M. P. A.; Trooster, J. M. *Nucl. Instrum. Methods* **1974**, *118*, 257–8.
(47) Calis, G. H. M.; Trooster, J. M.; Razi, M. T.; Sadler, P. J. *J. Inorg. Biochem.* **1982**, *17*, 139–145.
(48) Hill, D. T.; Sutton, B. M.; Isab, A. A.; Razi, T.; Sadler, P. J.; Trooster, J. M.; Calis, G. H. M. *Inorg. Chem.* **1983**, *22*, 2936–2942.

(SH titer < 0.06; 4.3 mM) were prepared in NH_4HCO_3 buffer. To 100 μL aliquots of each were added 10, 20, 30, 40, 50, or 60 μL of Et_3PAuSe-tagl (50 mM in MeOH). After 0.5 h of gentle stirring, the samples were chromatographed over Sephadex G-50 by using NH_4HCO_3 buffer. The ratio of gold bound to albumin (Au_b/BSA) and the SH titer of albumin were determined by analysis of the appropriate chromatographic fractions. Gold was quantitated by flame atomic absorption spectroscopy (AAS), albumin by its UV absorption at 278 nm (E_{278} = 39 600 L mol^{-1} cm^{-1}) and the albumin SH titer by using DTNB,[49] as previously described.[10]

Biological Assays of Anti-Inflammatory Activity. Phorbol Ester-Induced Inflammation. This assay was carried out following a previously published method used in evaluating AF.[50] Thus 1 mg of drug was dissolved in acetone (0.1 mL) and applied to the inner and outer surfaces of the right ear of Balb/c mice which had been treated 30 min before with 12-*O*-tetradecanoylphorbol acetate (TPA, 4 μg/20 μL). After 4 h the ear edema was evaluated using a thickness gauge and compared to the left ear which received only acetone. After euthanizing the animals with CO_2, the inflamed ear was removed and assayed for myeloperoxidase (MPO) activity as a measure of inflamed polymorphonuclear leukocytes.

Arachidonic Acid-Induced Inflammation. Details of the methodology used in this assay were described earlier.[51] Arachidonic acid (AA) (2 mg/20 μL) was applied to the inner surface of the left ear. The thickness of both left and right ears was measured 1 h after treatment, and the change in thickness between treated and untreated ear was recorded. The gold compounds (1 mg/ear) in acetone were given 15 min prior to AA. At the conclusion of the experiment (1 h) the animals were euthanized with CO_2, and the inflamed ear was removed and assayed for myeloperoxidase as a measure of polymorphonuclear leukocyte infiltration.

Carrageenan Rat Paw Edema Assay. The effect of SeAF on edema in the rat paw was measured in a manner similar to that employed earlier for the Et_3PAu(imido) complexes, according to a published procedure.[52,53] Doses of drug equivalent to between 15 and 20 mg of Au/kg of body weight were administered orally in tragacanth to male Charles River Lewis rats 1 h before subplantar injection of carrageenan into the right hind paw. The paw volume was determined after 3 h and compared to controls.

Gold Levels in Sera of Rats Dosed with Placebo, AF, or SeAF. Serum gold concentrations were determined by using a Varian Spectra AA-20 atomic absorption spectrophotometer equipped with a GT-96 graphite furnace tube atomizer and an auto sampler. The furnace was fitted with a plateau tube. The inert gas used was argon. The samples were diluted 20-fold into 1% v/v aqueous Triton X-100. The stock standard (998 ppm) was obtained from Inorganic Ventures, Lakewood, NJ. A series of working standards was prepared by diluting the stock standard into serum Triton X-100 solution to obtain a matrix equivalent to the samples. Standards were run at 0.02, 0.05, 0.10, 0.15, 0.20, 0.30, and 0.40 ppm. A blank was also prepared and analyzed. The method was validated by spiking sera samples or a serum blank with gold standard solution to cover the range of the standard curve. The range covered was equivalent to 0−8 ppm in the samples. Percentage recovery varied from 97 to 105% of theory.

Results and Discussion

Synthesis and Spectroscopic Characterization. The synthesis of SeAF is shown in Scheme 1 and was carried out in a manner similar to that used in making AF.[1] (For convenience in chemical equations, AF and SeAF are designated as Et_3PAuS-tagl and Et_3PAuSe-tagl, respectively, where tagl is tetraacetylglucose.) In the reaction of acetobromoglucose, however, selenourea was used in place of thiourea to give the known acetoglucose selenopseudourea hydrobromide required as an intermediate. Hydrolysis of this compound with aqueous potassium carbonate followed by coupling with chloro(triethylphosphine)gold(I) and purification via chromatography gave SeAF in 51% yield as a white crystalline solid. The β configuration at the anomeric carbon of SeAF follows from its mode of synthesis, which proceeds via the characterized intermediate hydrobromide as well as its ^{1}H, ^{13}C, and ^{31}P NMR spectra recorded in $CDCl_3$. All of these spectra are comparable in key aspects to the analogous NMR spectra of AF.[54]

Scheme 1

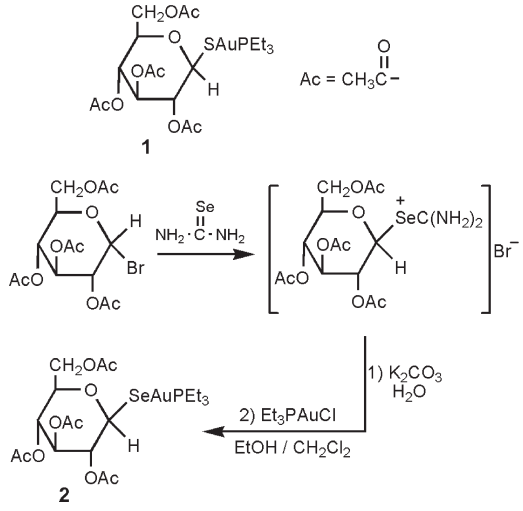

The proton-decoupled ^{31}P and ^{77}Se NMR spectra both yielded singlets for SeAF in chloroform solution. The ^{31}P NMR spectra in methanol, DMSO, and 1:1 MeOH:H_2O obtained during the protein studies (vide infra) also exhibited only a singlet for SeAF. Sadler earlier observed ^2J coupling of ^{31}P to ^{15}N through gold in ^{15}N-enriched phosphine gold(I) phthalimide complexes of 41 and 43 Hz for Et_3P and $(C_6H_5)_3P$, respectively.[53] Hormann and Shaw observed $^2J_{PC}$ coupling in aliphatic $R_3PAu^{13}CN$ complexes (R = Me, Et, *i*Pr, and Cy) at room temperature, whereas ligand scrambling obscured the coupling in Ph_3PAu-CN at room temperature but not at 200 or 240 K in methanol.[41,55] However, $^2J_{PSe}$ coupling through gold between ^{31}P and ^{77}Se was not observed in the NMR spectra of either nuclei at ambient temperature in chloroform or by ^{31}P NMR in methanol, DMSO, or 1:1 MeOH:H_2O. Variable temperature ^{31}P{^{1}H} experiments likewise failed to reveal $^2J_{PSe}$ coupling through gold(I). In $CDCl_3$ at −27 °C the single line broadened to ca. 20 Hz at half height, and the chemical shift moved upfield by ~150 Hz (1 ppm). In CD_3OD, the temperature was varied incrementally to −73 °C, resulting in an upfield shift of 5.5 ppm and line broadening to 120 Hz. Two-bond selenium−phosphorus coupling ($^2J_{PSe}$) may exhibit either positive or negative values.[56] Coupling across gold

(49) Ellman, G. *Arch. Biochem. Biophys.* **1959**, *82*, 70–77.
(50) Carlson, R. P.; O'Neill-Davis, Chang, J.; Lewis, A. J. *Agents Actions* **1985**, *17*, 197–204.
(51) Griswold, D. E.; Webb, E.; Schwartz, L.; Hanna, N. *Inflammation* **1987**, *11*, 189–199.
(52) Walz, D. T.; DiMartino, M. J.; Griffin, C. L.; Misher, A. *Arch. Int. Pharmacodyn. Ther.* **1970**, *185*, 337–343.
(53) Berners-Price, S. J.; DiMartino, M. J.; Hill, D. T.; Kuroda, R.; Mazid, M. A.; Sadler, P. J. *Inorg. Chem.* **1985**, *24*, 3425–3424.
(54) Razi, M. T.; Sadler, P. J.; Hill, D. T.; Sutton, B. M. *J. Chem. Soc., Dalton Trans.* **1983**, 1331–1334.
(55) Hormann, A. L.; Shaw, C. F., III. *Inorg. Chem.* **1990**, *29*, 4683–4687.
(56) Duddeck, H. *Prog. Nucl. Magn. Reson. Spectrosc.* **1995**, *27*, 1–323.

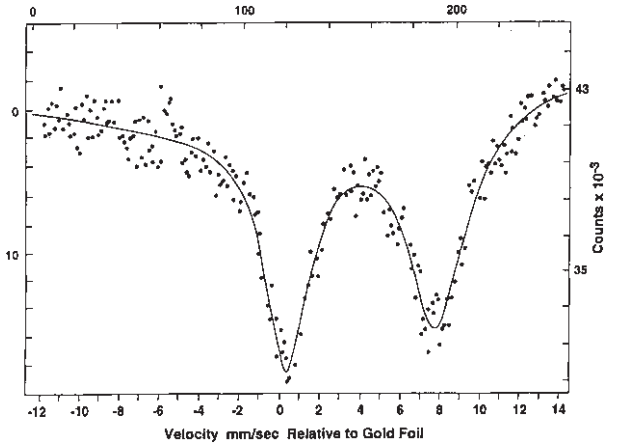

Figure 1. ^{197}Au Mössbauer spectrum of SeAF at 4.2 K; IS = 0.0 for gold foil.

has been observed in only three cases, (2,4,6-tri*t*-butylphenylselenide)(triphenylphosphine)gold(I), $^{2}J_{PSe} = \pm 41$ Hz;[30] $[Ph_3PAu\{SeC(NH_2)_2\}]Cl$, $^{2}J_{PSe} = -13$ Hz;[31] and $[(\mu\text{-dppm})(AuSeC(NH_2)_2)_2]Cl_2$, $^{2}J_{PSe} = -13$ Hz.[32] No $^{2}J_{PSe}$ coupling was reported for 28 additional compounds with P−Au^{I}−Se coordination reviewed by Molter and Mohr,[37] including Beck et al.'s[38] earlier report of SeAF. The absence of coupling may reflect scalar coupling values that are less than the line widths of the ^{31}P (7 Hz in both $CDCl_3$ and CD_3OD) or ^{77}S (ca. 3.5 Hz) resonances observed at room temperature. The broadening observed at low temperature may result from viscosity effects and/or dissociation or exchange equilibria for the phosphine and/or selenoglucose ligand. The ESI-MS studies below address this issue.

Mössbauer Spectroscopy. The gold-197 Mossbauer spectrum of SeAF was obtained at 4.2 K and is exhibited (Figure 1) as an asymmetric quadrupole doublet. This asymmetry is indicative of residual sample texture, i.e., nonrandom orientation of the principal component of the electric field gradient tensor at the gold centers with respect to the direction of propagation of the 77.3 keV Mössbauer γ ray of ^{197}Au. Both the isomer shift (IS) and quadrupole splitting (QS) of SeAF values are fairly typical of linear Au^{I} in the solid state but are smaller than those obtained for AF measured by us under the same conditions: IS 4.03 and QS 7.40 mm s^{-1} for SeAF compared to 4.89 and 8.69 mm s^{-1}, respectively, for AF. The latter values for AF are comparable to those reported in the literature.[48] The smaller IS and QS values for SeAF indicate less distortion in the Se−Au and Au−P bonds and more covalent character than the S−Au and Au−P bond of AF. This is consistent with the fact that selenium is a softer Lewis base.

XANES and EXAFS. Both the gold oxidation state and the presence of Au−P bonds produce readily identifiable patterns in the X-ray absorption near-edge structure (XANES) spectrum.[57] Gold(I) lacks a peak for the 2p−5d transition that predominates the XANES region of Au(III) species and does not have the recognizable peaks at 11 945 and 11 967 eV that are seen in this region for Au metal. Complexes which contain Au−P bonding exhibit a peak at 11 928 eV whose magnitude is directly proportional to the number of bound phosphorus atoms.

(57) Elder, R. C.; Eidsness, M. K. *Chem. Rev.* **1987**, *87*, 1027–1046.

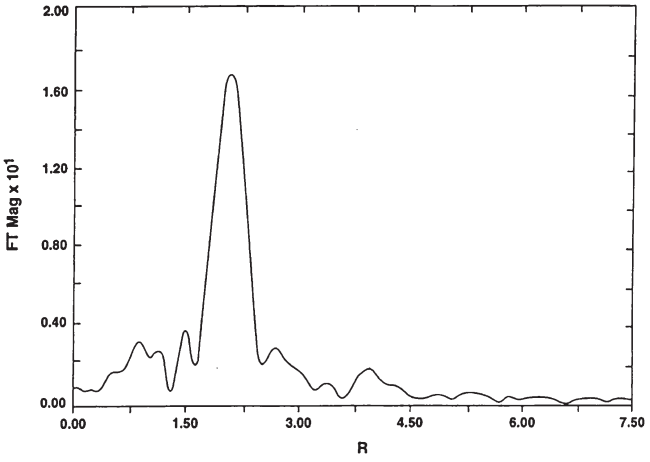

Figure 2. FT Au EXAFS spectrum (in phase-shifted angstrom space) of SeAF. The peak was fit to a combination of P and Se scattering at 2.28 and 2.41 Å, respectively.

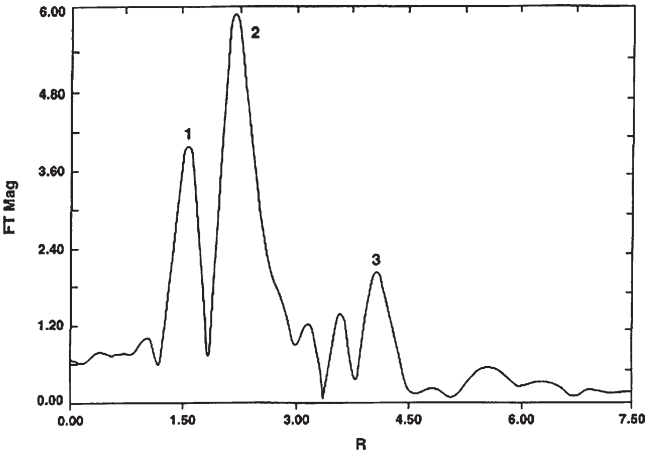

Figure 3. FT Se EXAFS spectrum (in phase-shifted angstrom space) of SeAF. Peaks 1−3 arise from C, Au, and, due to the linear geometry at Au, P at distances of 1.91, 2.39, and 4.61 Å.

Based on the peak intensity at 11 928 eV in the XANES spectrum, SeAF appears to have a central Au atom in the +1 oxidation state with a single phosphorus ligand bound to it (consistent with the Mössbauer spectrum).

EXAFS data were measured at both the gold and selenium absorption edge energies to determine the local environment for both atoms. Figure 2 shows the Fourier transform (FT) for the data measured at the gold edge. A single intense peak is present at 2.0 Å in the filtered EXAFS (Ff). Curve fitting to the Ff from this peak using a single shell of either phosphorus or selenium was found to be inadequate. This is due in part to the large Z difference between the phosphorus and selenium donors. A much better fit was achieved by assuming that the peak arises from both phosphorus and selenium donors. The results are 0.9 phosphorus atoms at 2.28 Å and 1.6 selenium atoms at 2.41 Å.

Three distinct peaks are present in the FT for the data measured at the selenium edge energy (Figure 3). The filtered EXAFS extracted from first peak was fit as a carbon donor. The results of this fit are 1.2 carbon atoms at 1.91 Å. In accordance with the Ff from the data at the gold edge energy, the filtered EXAFS from the main peak was fit as a Se−Au bond. The results for the calculation were 0.9 Au atoms at a distance of 2.39 Å. The third peak

in Figure 2 is attributed to the second-shell phosphorus atom, which results from the colinearity of the Au−P and Au−Se bonds. The curve fitting to the filtered EXAFS from this peak gave 1.4 phosphorus atoms at a nonbonded distance of 4.61 Å.

The results from the gold and selenium edge energy data are in close agreement. First, the Au−Se bond distances determined by Au and Se EXAFS differ only by 0.02 Å. Second, the sum of the Au−P and Au−Se bond distances calculated from the gold edge data is 4.69 Å, which is in moderate agreement with the nonbonded distance of 4.61 Å resulting from the fit to a phosphorus donor from the selenium edge data. This also indicates that there is a nearly linear angle ∠P−Au−Se, which is consistent with the present Mössbauer spectrum and many known gold(I) structures.[57,58] The EXAFS bond distances are in good agreement with the average Au−Se and Au−P bond lengths, 2.418 ± 0.007 and 2.269 ± 0.006 Å based on six structures (Ar_3-PAuSeR′) having triarylphosphine and selenol ligands with 9 independent, linear P−Au−Se groupings retrieved from the Cambridge Crystallography Database.[58] The structure implied by the EXAFS and Mössbauer results is also in good agreement with the crystallographically determined structure of AF,[59] which has a sulfur atom in place of the selenium.

Electrospray Ionization Mass Spectrometry. Positive- and negative-ion spectra were obtained on 5.0 mM samples in MeOH:H_2O solvent to determine whether scrambling to cationic and anionic species was occurring in solution. The positive-ion spectra (Figure 4a,b) included dominant signals for $[(Et_3P)_2Au]^+$ exhibiting the parent ion (m/z = 433 and an M + 1 ^{13}C signal); $[(Et_3PAu)_2Se\text{-tagl}]^+$ (m/z = 1041, ^{80}Se) exhibiting the expected six component Se isotopic signature (^{74}Se, ^{76}Se, ^{77}Se, ^{78}Se, ^{80}Se, and ^{82}Se at 1.8, 18.9, 15.4, 47.9, 100, and 17.6 abundances relative to ^{80}Se with superimposed M + 1 ^{13}C signals, see Supporting Information, Figure S1), and $[(Et_3PAu)_3Se\text{-tagl}]^+$ (m/z = 1357). Protonated seleno-auranofin $[SeAF-H]^+$ and weaker sodiated and potassiated signals (m/z = 727, 749, 765, ^{80}Se) were also observed (Figure 4a). In the negative-ion spectrum, a single peak for $[Au(Se\text{-tagl})_2]^-$ (m/z = 1019 $^{80}Se_2$, pattern characteristic of a diselenium species, see Supporting Information, Figure S2) was observed (Figure 4c). The signals for the $[(Et_3P)_2Au]^+$ and $[Au(Se\text{-tagl})_2]^-$ are strong and unlikely to be artifacts of the electrospray desolvation process, unlike the weaker protonated, sodiated, and potassiated seleno-auranofin signals. Thus, the mass spectra provide evidence for scrambling of the Et_3P and tagl-Se^- ligands in solution according to eq 1a:

$$2Et_3PAuSe\text{-tag1} \rightleftharpoons [(Et_3P)_2Au]^+ + [Au(Se\text{-tag1})_2]^- \quad (1a)$$

The $[(Et_3PAu)_2(Se\text{-tagl})]^+$ ion can form by a reaction of two SeAF molecules with displacement of a seleno-tetraacetyl-glucose ligand according to eq 1b:

$$2Et_3PAuSe\text{-tag1} + H^+ \rightleftharpoons [(Et_3PAu)_2Se\text{-tag1}]^+ + \text{tag1-SeH} \quad (1b)$$

Equilibrium scrambling, analogous to eq 1a, has been reported for many classes of two-coordinate mixed-ligand gold(I) species, $[YAuX]^{+/0/-}$ that exist in equilibrium with the related homoleptic complexes, $[AuY_2]^{\pm}$ and $[AuX_2]^{\pm}$.

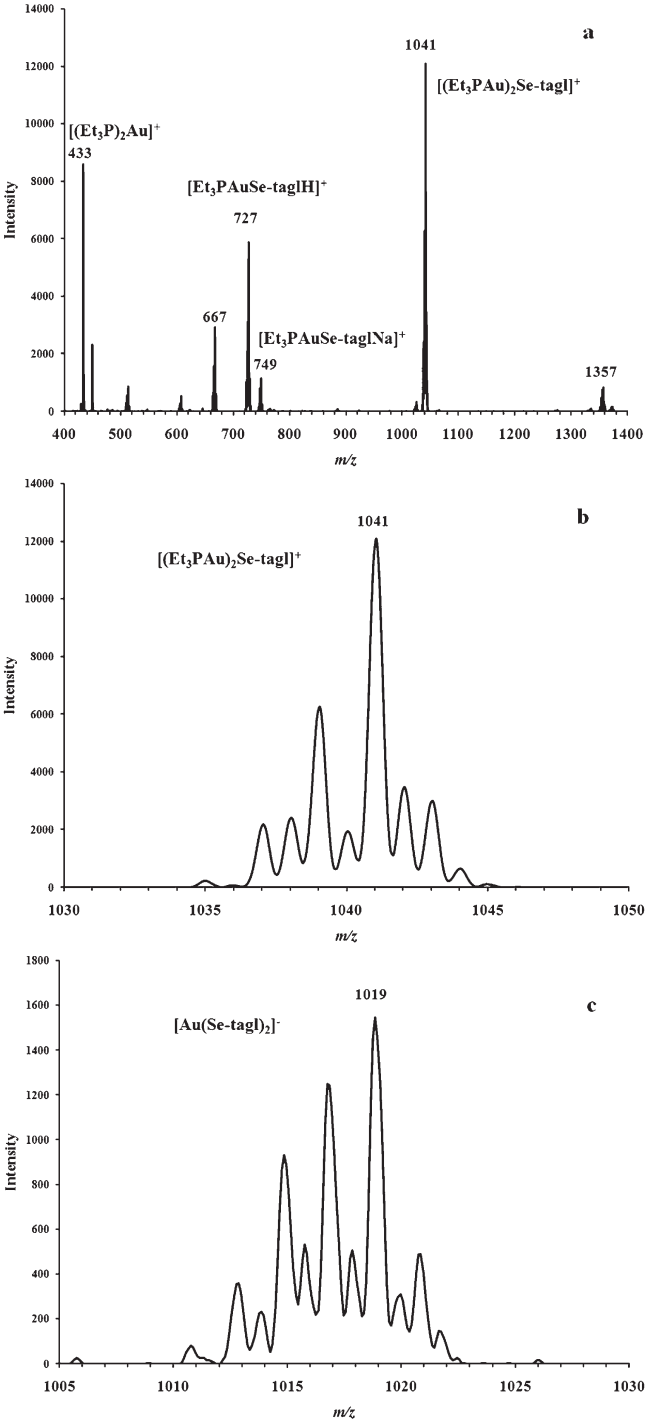

Figure 4. ESI-MS spectra of SeAF (10 mM in 1:1 MeOH:H_2O): (a) positive-ion spectrum; (b) isotope pattern for $[(Et_3PAu)_2Se\text{-tagl}]^+$ (m/z = 1041, ^{80}Se); (c) negative-ion isotope pattern for $[Au(Se\text{-tagl})_2]^-$ (m/z = 1019, $^{80}Se_2$).

(58) (a) SIHPOO: Jones, P. G.; Thone, C. *Chem. Ber.* **1990**, *123*, 1975–1978. (b) LECTUI, LECVIY: Eikens, W.; Kienitz, W. C.; Jones, P. G.; Thone, C. *J. Chem. Soc., Dalton Trans.* **1994**, 83–90. (c) UMUJIV: Canales, S.; Crespo, O.; Gimeno, M. C.; Jones, P. G.; Laguna, A.; Romero, P. *J. Chem. Soc., Dalton Trans.* **2003**, 4525–4528. (d) OKANIX: Schneider, D.; Nogai, S.; Scheier, A.; Schmidbaur, H. *Inorg. Chim. Acta* **2003**, *352*, 179–187. (e) MESYEP: Laromaine, A.; Teixidor, F.; Kivekas, R.; Sillanpaa, R.; Arca, M.; Lippolis, V.; Crespo, E.; Vinas, C. *J. Chem. Soc., Dalton Trans.* **2006**, 5240–5247.

(59) Hill, D. T.; Sutton, B. M. *Cryst. Struct. Commun.* **1980**, *9*, 679–686.

The equilibrium constant for scrambling is defined as $K_S = [AuX_2][AuY_2]/[YAuX]^2$. If the extent of scrambling is purely statistical, $K_S = 0.250$; larger values indicate that the homoleptic complexes are favored, whereas a lower value indicates that the mixed-ligand complex is favored. The initial reports,[60,61] beginning in 1985−1986, were primarily qualitative. The cyano(thiomalato)gold(I) complex, [TmSAuCN]$^{3-}$, characterized by ^{13}C NMR,[60,61] ^{15}N NMR,[62] and Raman spectroscopy[60] in aqueous solution, exists in equilibrium with $[Au(CN)_2]^-$ and $[Au(STm)_2]^{5-}$; the mono- and dicyano species were resolved in the ^{13}C and ^{15}N NMR spectra.[60,61] The analogous complexes of glutathione ([GtSAuCN]$^{2-}$),[60] thioglucose ([TgSAuCN]$^-$),[60,63] and thiosulfate ($[Au(CN)(S_2O_3)]^{2-}$)[64] also equilibrate to form the dicyanoaurate(I) and bis(thiolato)aurate(I) or bis(thiosulfato)aurate(I) complexes. [Et_3PAuCN] is a molecular solid, but concomitant observation of the signals for $[(Et_3P)_2Au]^+$ and $[Au(CN)_2]^-$ in solution by ^{31}P and ^{13}C NMR demonstrated the scrambling equilibrium.[41,55] ESI-MS spectra of [Et_3PAuCN] and [Me_3PAuCN] in solution exhibit strong signals for $[Au(CN)_2]^-$ and the respective $[(R_3P)_2Au^+]$ cations (J.W. Webb and C.F. Shaw III, unpublished observations). When the mixed-ligand complex is neutral, the homoleptic complexes are oppositely charged and, therefore, solvent effects should be significant. [Et_3PAuCN], the first case for which K_S values were reported, exhibits increasing extent of scrambling in polar solvents at room temperature (with esd values): $CDCl_3$, $K_S = 0.018$ (0.004); C_6D_6, $K_S = 0.034$ (0.008); $(CD_3)_2SO$, $K_S = 0.092$ (0.004); and CH_3OD, $K_S = 0.20$ (0.06).[41,55] Yet, scrambling does occur in the less-polar solvents, benzene and chloroform (the solvent used for SeAF NMR studies), as well as more-polar solvents. In contrast, at 297 K, [Ph_3PAuCN] undergoes rapid exchange with $[(Ph_3P)_2Au]^+$ and $[Au(CN)_2]^-$, yielding only a single resonance in the ^{13}C and ^{31}P NMR spectra, but at 200−240 K the respective ^{13}C and ^{31}P NMR signals were observed for the homoleptic ionic species ($K_s = 0.112$ (0.005) at 240 K). K_s values were measured for four trialkylphosphine analogues, which in methanol exhibited resolved ^{31}P and ^{13}CN resonances for $[(Et_3P)_2Au]^+$ and $[Au(CN)_2]^-$, respectively, at 298 and 240 K. The K_s values, measured at 240 K for comparison to the phenyl analogue, are [Me_3PAuCN], $K_s = 0.37$ (0.05); [Et_3PAuCN], $K_S = 0.24$ (0.02); [iPr$_3$PAuCN], $K_S = 0.29$ (0.03); and [Cy_3PAuCN], $K_S = 0.49$ (0.02).[41,55]

The equilibrium constants of four inorganic species in aqueous solution, initially reported as K_{RD} for the reaction in the reverse sense (i.e., $K_S = K_{RD}^{-1}$), were determined using electronic spectroscopy for [Au(CN)(mpt)], $K_S = 3.16$[65] or calculated from related equilibrium constants for [Au{$(H_2N)_2$CS}I], $K_S = 0.63$;[65,66] [Au(CN)I]$^-$, $K_S = 0.50$;[65,67] and [Au(SCN)I]$^-$, $K_S = 0.50$.[65,68] DMSO dissolves solid AuCN to form both $[Au(CN)_2]^-$ and [(DMSO)AuCN],[69] indicative of scrambling by the latter compound. Selenocyanate undergoes a complex set of reactions with gold(I) thiomalate $[\{Au(STm)\}_n]^{2n-}$, producing inter alia [TmSAuSeCN]$^{3-}$,[36] which scrambles to form $[Au(STm)_2]^{5-}$ and $[Au(SeCN)_2]^-$, which slowly decomposes to selenium and $[Au(CN)_2]^-$.

Equilibrium scrambling constants for a series of cyano(imidazoladine-2-thione)gold(I) complexes,[69] [(RR′Imt)AuCN], have been determined for [(Imt)AuCN] in DMSO, $K_S = 0.630$ (0.005) and in methanol, $K_s = 0.47$, and in DMSO for [(MeImt)AuCN], $K_S = 0.56$ (0.02); [(EtImt)AuCN], $K_S = 0.62$ (0.01); [(nPrImt)AuCN], $K_S = 0.59$ (0.01); [(iPrImt)AuCN], $K_S = 0.55$ (0.01); [(Diaz)AuCN], $K_S = 0.91$ (0.01); and [(Diap)AuCN], $K_S = 0.96$ (0.01).[69] All are larger than the statistical value, which indicates that formation of the ionic products is somewhat favored in solution. The constant measured in aqueous solution for [(ErgS)AuCN] ($K_S = 1.08$)[70] reflects the more-polar aqueous environment.[70]

K_S values were measured in DMSO for a similar series of cyano(imidazoladine-2-selenone)gold(I) complexes, [(RR′ImSe)AuCN], [(ImSe)AuCN], $K_S = 2.95$ (0.05); [(MeImSe)AuCN], $K_S = 2.90$ (0.08); [(EtImSe)AuCN], $K_S = 2.76$ (0.06); [(i-PrImSe)AuCN], $K_S = 3.12$ (0.02); [(PhImSe)AuCN], $K_S = 4.28$ (0.05); [(Et_2ImSe)AuCN], $K_S = 2.84$; and [(DiazSe)AuCN], $K_S = 3.64$ (0.06).[32] The K_S values for the imidazolidine-2-selenone complexes are typically 4−5 times greater in value for the corresponding imidazolidine-2-thione, indicating that for selenones, the scrambling equilibrium lies farther to the right.[32]

Scrambling of [Cy_3PSeAuCN] ($K_S = 1.81$) and [Cy_3PSAuCN] ($K_S = 0.147$) in methanol has been observed by ^{13}C NMR,[33,34] but in the ^{31}P NMR spectra, only singlets, consistent with rapid exchange of the phosphine ligand between $[Au(PEt_3)_2]^+$ and the parent compound, are observed. In this case, K_S for the selenophosphine complex is more than an order of magnitude greater than for the thiophosphine derivative.[33]

Et_3PAuSTg (deacetylated auranofin) in CH_3OD and in 1:3 CH_3OH:D_2O exhibits ^{31}P resonances characteristic of [(Et_3PAuSTg)] and $[(Et_3P)_2Au]^+$. The latter increased in intensity in the more polar MeOH:H_2O mixture. Auranofin itself, like selenoauranofin, exhibits a single resonance at ambient temperature, that was not resolved at lower temperature.[41b]

Nine neutral compounds having an empirical formula, YAuX, have been characterized crystallographically as ionic solids consisting of homoleptic two-coordinate gold(I) cations and anions: $[\{(NC(CH_2)_2)_3P\}_2Au][Au(CN)_2]$,[71] $[Au\{(CH_3NH)_2C{=}S\}_2][Au(CN)_2]$,[72] $[(THT)_2Au][AuI_2]$,[73] $[(TPA)_2Au][Au(CN)_2]$,[74] $[(Imt)_2Au][AuI_2]$,[75]

(60) Lewis, G.; Shaw, C. F., III. *Inorg. Chem.* **1986**, *25*, 58–62.
(61) Graham, G. G.; Bales, J. R.; Grootveld, M. C.; Sadler, P. J. *J. Inorg. Biochem.* **1985**, *25*, 163–173.
(62) Isab, A. A.; Gazi, I. H.; Wazeer, M. I. M.; Prezanowski, H. P. *J. Inorg. Biochem.* **1993**, *50*, 299–304.
(63) Isab, A. A. *J. Inorg. Biochem.* **1992**, *46*, 145–151.
(64) El-Hinnawi, M. A.; Peter, L.; Meyer, B. *J. Raman Spectrosc.* **1985**, *16*, 272–279.
(65) Dickson, P. N.; Wherli, A.; Geier, G. *Inorg. Chem.* **1988**, *27*, 2921–2925.
(66) Belevantsev, V. I.; Peshchevitskii, B. I.; Tsvelodub, L. D. *Neorg. Khim.* **1986**, *31*, 3065–3068. *Russ. J. Inorg. Chem.* **1986**, *31*, 1762-1763
(67) Belevantsev, V. I.; Peshchevitskii, B. I.; Tsvelodub, L. D. *Neorg. Khim.* **1987**, *32*, 108–112. *Russ. J. Inorg. Chem.* **1987**, *32*, 59-61.
(68) Belevantsev, V. I.; Peshchevitskii, B. I.; Tsvelodub, L. D. *Izv. Sib. Otd. Akad. Nauk SSSR, Ser. Khim. Nauk* **1985**, 64–70.
(69) Ahmad, S.; Isab, A. A.; Perzanowski, H. P. *Can. J. Chem.* **2002**, *80*, 1279–1284.
(70) Ahmad, S.; Isab, A. A. *Inorg. Chem. Commun.* **2001**, *4*, 362–364.
(71) Hussein, M. S.; Al-Arfaj, A. R.; Akhtar, A. A.; Isab, A. A. *Polyhedron* **1996**, *16*, 2781–2785.
(72) Stocker, F. B.; Britton, D. *Acta Crystallogr., Sect. C: Cryst. Struct. Commun.* **2000**, *C56*, 798–800.
(73) Ahrland, S.; Noren, B.; Oskarsson, A. *Inorg. Chem.* **1985**, *24*, 1330–1333.
(74) Assefa, Z.; Omary, M. A.; McBurnett, B. G.; Mohamed, A. A.; Patterson, H. H.; Staples, R. J.; Fackler, J. P., Jr. *Inorg. Chem.* **2002**, *41*, 6274–6280.
(75) Friedrichs, S.; Jones, P. G. *Acta Crystallogr.* **1999**, *C55*, 1625–1627.

$[(Ad_2BzP)_2Au][Au(CN)_2]$,[76] $[(Me_2PhP)_2Au][Au(GeCl_3)_2]$,[77] $[(Ph_3P)_2Au][Au(S(=O)_2\text{-}p\text{-}Tol)_2]$,[78] and $[(3\text{-}BrPy)_2Au][AuCl_2]$.[79] Spectroscopic evidence also supports ionic formulations for two isocyanide compounds, $[(RNC)_2Au][AuS(=O)_2\text{-}p\text{Tol}]$, (R = *t*Bu, 2,6-$Me_2C_6H_3$),[78] and five alkyl-substituted imidazolidine-2-selenone complexes, $[(RR'ImSe)_2Au][Au(CN)_2]$, R, R′ = Et_2; Et,H; Me,H; *i*Pr,H; and Ph,H.[32] The equilibrium scrambling constant for $[Au\{(CH_3NH)_2C{=}S\}_2][Au(CN)_2]$ has been measured ($K_S = 0.98(0.03)$), demonstrating the reversibility of the scrambling process,[72] i.e., the homoleptic ionic complexes equilibrate in solution to form the neutral species. The ionic selenones also exhibited separate ^{13}CN resonances for $[Au(CN)_2]^-$ and [R,R′ImSeAuCN], further demonstrating that the scrambling process for the gold(I) species is reversible.

This extensive array of gold(I) complexes known to undergo scrambling in solution, including the thiolato auranofin analogue [$Et_3PAuSTg$], reinforced by the multiple examples of imidazolidine-2-selenone and triethylphosphine selenide complexes that exhibit a greater extent of scrambling, and therefore larger K_S values, than the sulfur analogues, strongly supports the ESI-MS evidence for the equilibrium scrambling of selenoauranofin according to eqs 1a and 1b.

The observation of $[(Et_3P)_2Au]^+$ and $[Au(Se\text{-}tagl)_2]^-$ in the ESI-MS spectra, but not by NMR, suggests that the absence of $^2J_{PSe}$ scalar coupling in the ^{31}P and ^{77}Se NMR spectra may arise in part from a labile exchange process in solution. $^2J_{PSe}$ coupling is routinely observed in square planar Pt(II) compounds and is typically larger for trans orientation of the Se and P donor atoms than the cis orientation.[56,80−82] For example, Pan and Fackler observed $J_{PSe,trans} = -100$ and $J_{PSe,cis} = -10$ Hz for $[Pt(Se_2CN{-}iBu_2)(PPh_3)Cl]$, and $J_{PSe,trans} = -100.5$ and $J_{PSe,cis} = -10$ Hz for $[(Se_2CN{-}Et_2)(PPh_3)Cl]$.[80] For *cis*-$[Pt(\kappa^2\text{-}Ph_2P'{-}CH_2{-}P''Ph_2(=Se)(PEt_3)Cl]^+$ and *trans*-$[Pt(\kappa^2\text{-}Ph_2P'{-}CH_2{-}P''Ph_2(=Se)(PBu^n_3)Cl]^+$ (cis and trans are defined by the relationship of the Se and Cl^- donor atoms)[82] Berry et al. observed coupling between the PR_3 ligand and Se, $J_{PSe,trans} = \pm 102.9$ and $J_{PSe,cis} = \pm 20$ Hz, respectively.[82] Interestingly, there are cases where the coupling has been observed for a Pt compound but not for the analogous Pd(II) or Ni(II) compound:[80,82] For example, Pan and Fackler[80] observed no J_{PSe} coupling for $[Pd(Se_2CN{-}iBu_2)(PPh_3)Cl]$ or $[Ni(Se_2CN{-}Et_2)(PPh_3)Cl]$, which are analogues of the Pt diselenocarbamates just described. Similarly, Berry et al[82] observed that $^2J_{PSe,cis}$ was not observed for *trans*-$[Pd(\kappa^2\text{-}Ph_2P'{-}CH_2{-}P''Ph_2(=Se)(PEt_3)Cl]^+$, although the cis complex exhibits $J_{PSe,trans} = \pm 125$ Hz. Pt(II) is inert to ligand exchange, whereas Pd(II) and Ni(II) are both labile metal centers, thus providing a precedent for loss of observable coupling in labile systems, such as gold(I), where in only 3 of 31 instances was coupling resolved.[37]

Biomimetic Albumin-Binding Studies. Human serum albumin is the principle gold transport agent in the blood.[9] It is a microheterogeneous protein which consists principally of mercaptalbumin ($AlbS^-$) in which the acidic cysteine-34 residue is in the reduced state and in an oxidized, disulfide form in which cysteine 34 is linked to a nonprotein cysteine residue (AlbSSCy). Bovine serum albumin (BSA) was used in preference to human albumin because it has a greater and more reliable content of mercaptalbumin ($AlbS^-$), which binds gold most avidly[10,83] due to the low pK_{SH} value (∼5) of cysteine-34. (To clarify the discussion, microheterogeneous preparations of albumin will be designated BSA, whereas individual molecular species will be designated as $AlbS^-$ and AlbSSCy, etc. Two modified preparations, Ac-BSA and Cy-BSA, in which the reduced cysteine-34 residues are converted to a thioether and a disulfide, respectively, are described below.) The reactions of $Et_3PAuSe\text{-}tagl$ with BSA were examined using ^{31}P NMR spectroscopy, size-exclusion (gel permeation) chromatography to resolve free (i.e., low-molecular-weight) and protein-bound gold, and DTNB analysis of the albumin thiol content. The amino-acid sequences of mammalian albumins contain a total of 35 conserved cysteine residues, of which the remaining 34 form 17 "internal" disulfide linkages. The experiments described below were performed using a single source of BSA with a thiol titer ($[AlbS^-]/[BSA]_{total}$) of 0.56. This value is close to the in vivo range of 0.6−0.7, which indicates that minimal oxidation of Cys-34 had occurred during the preparation and storage of the albumin. The interpretation of the reactions of Se-AF with albumin depends, in part, on extensive studies[9−14,83−85] employing ^{31}P NMR (Table 1), Mössbauer, and EXAFS spectroscopies, combined with protein modification and analysis of bound gold and reduced thiol status, in order to characterize the gold species formed by reactions of auranofin, gold thiomalate, and related compounds at: (i) cysteine-34, (ii) cysteine residues generated by reduction of internal disulfide bonds, and (iii) the numerous histidine residues present in albumin.[11−14,83−85] Ralph et al. recently confirmed the various gold binding modes by ESI-MS.[86]

Preliminary to the present albumin studies, ^{31}P NMR chemical shifts of $Et_3PAuSe\text{-}tagl$ were determined in DMSO and CH_3OD and, by adding a concentrated methanolic solution, in the aqueous buffer (l00 mM NH_4HCO_3, pH 7.9) used for the protein chemistry (Table 1). The δ_P falls between 37.7 and 37.9 ppm in these solvents. The spectrum obtained in the methanol/buffer solution is shown in Figure 5a.

Two successive aliquots of $Et_3PAuSe\text{-}tagl$ were added to BSA to generate mixtures with Au/BSA stoichiometric ratios of 0.25 and 0.48. ^{31}P NMR resonances observed at 38.6 and 61.2 ppm after the first addition (Figure 5b) increased in intensity with the second aliquot (Figure 5c). The 38.6 ppm resonance is due to $AlbSAu{-}PEt_3$[11−14] formed at cysteine-34 according to eq 2:

$$AlbS^- + Et_3PAuSe\text{-}tag1 + H^+ \rightleftharpoons AlbSAuPEt_3 + tag1\text{-}SeH \quad (2)$$

(76) Monkwius, U.; Zabel, M.; Yersin, H. *Inorg. Chem. Commun.* **2008**, *11*, 409–412.
(77) Bauer, A.; Schmidbaur, H. *J. Am. Chem. Soc.* **1996**, *118*, 5324–5325.
(78) Römbke, P.; Schier, A.; Schmidbaur, H. *J. Chem. Soc., Dalton Trans.* **2001**, 2482–2486.
(79) Freytag, M.; Jones, P. G. *Chem. Commun.* **2000**, 277–278.
(80) Pan, W.-H.; Fackler, J. P., Jr. *J. Am. Chem. Soc.* **1978**, *100*, 5783–5789.
(81) Pietschnig, R.; Moser, C.; Spirk, S.; Schäfer, S. *Inorg. Chem.* **2005**, *45*, 2798–2802.
(82) Berry, E. E.; Browning, J.; Dixon, K. R.; Hilts, R. W. *Can. J. Chem.* **1988**, *66*, 1272–1282.
(83) Isab, A. A.; Hormann, A. L.; Coffer, M. T.; Shaw, C. F., III. *J. Am. Chem. Soc.* **1988**, *110*, 2278–2284.
(84) Xiao, J.; Shaw, C. F., III. *Inorg. Chem.* **1992**, *31*, 3706–3710.
(85) Kinsch, E. M.; Stephan, D. W. *Inorg. Chim. Acta* **1984**, *91*, 263–267.
(86) Talib, J.; Beck, J. L.; Ralph, S. F. *J. Biol. Inorg. Chem.* **2006**, *11*, 559–570.

Table 1. ^{31}P NMR Chemical Shifts[a] of Seleno-Auranofin, Analogues, and Reaction Products

species	solvent	δ_P/ppm[b]	refs
Et_3PAuSe-tagl	100 mM NH_4HCO_3 buffer	37.8 ± 0.1	[c]
Et_3PAuSe-tagl	DMSO-d_6	37.83	[c]
Et_3PAuSe-tagl	CD_3OD-d_4	37.80	[c]
Et_3PAuS-tagl	100 mM NH_4HCO_3 buffer	37.0 ± 0.3	14
Et_3PAuCN	100 mM NH_4HCO_3 buffer	35.4 ± 0.1	36
$Et_3PAuSCy$	100 mM NH_4HCO_3 buffer	36.6 ± 0.01	
$[(Et_3P)Au]^+$	100 mM NH_4HCO_3 buffer	44.0 ± 0.4	10b, 15
$Et_3P{=}O$	100 mM NH_4HCO_3 buffer	61.5 ± 0.5	10b, 14, 36
$AlbSAuPEt_3$[d]	100 mM NH_4HCO_3 buffer	38.6 ± 0.2	10b, 14, 36, 37
$(Et_3PAuS)_x$BSA [d]	100 mM NH_4HCO_3 buffer	33−37	10b,
Et_3PAuN_{His}-BSA [d]	100 mM NH_4HCO_3 buffer	23−30	37
$AlbS(AuPEt_3)_2$[d]	100 mM NH_4HCO_3 buffer	35.7 ± 0.1	14, 37

[a] Chemical shift values were measured and are reported vs internal TMP (2.74 ppm vs H_3PO_4). [b] Error limits reflect variations observed in protein solutions; ranges are given for binding sites that occur in multiple protein environments. [c] This work. [d] Microheterogeneous commercial and modified albumin samples are designated using "xx-BSA" and contain two or more different albumin species. The individual, albumin molecules dependent on the status of cysteine-34 are abbreviated using "AlbS-xxx".

The 61.2 ppm resonance is due to Et_3PO formed via the displacement (eq 3a or 3b) and subsequent oxidation (eq 4) of the phosphine ligand by disulfide bonds.[11]

$$AlbS^- + Et_3PAuSe\text{-tagl} \rightleftharpoons [AlbSAuSe\text{-tagl}] + Et_3P \quad (3a)$$

$$AlbSAuPEt_3 + tag1\text{-}SeH \rightleftharpoons [AlbSAuSe\text{-tagl}]^- + Et_3P + H^+ \quad (3b)$$

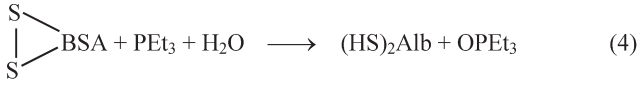

(4)

The transformations of eqs 2, 3a, and 3b can occur via a three-coordinate transition state (Scheme 2), analogous to that previously discussed for interactions of Et_3PAuCN with cyanide and $AlbS^-$ with Et_3PAuCN, which also leads to extensive displacement of Et_3P and its subsequent oxidation.[83] Displacement of Et_3P from $AlbSAuPEt_3$ by thiols has been documented previously[11] and increases with the affinity of the thiol for gold.[11a] Thus displacement by tagl-Se (eqs 3a, 3b) can be reasonably anticipated, given the greater affinity of selenium ligands for gold(I) compared to the analogous thiols.[15] Analogues of AlbSAuSe-tagl with thiol ligands, AlbSAuSTm[10a] and AlbSAuS-tagl,[14] were isolated and characterized by their gold and thiol contents, XANES, and EXAFS spectroscopy, and AlbSAuSTm was also characterized by Mössbauer spectroscopy.

When the Et_3PAuSe-tagl:BSA ratio reached 0.89 (Figure 5d), the cysteine-34 thiolate (0.56 per mole of albumin) became saturated, and a resonance at 37.8 ppm appeared due to excess Et_3PAuSe-tagl. The minor resonance at 43.7 ppm is assigned to $[(Et_3P)_2Au]^+$, which forms via ligand scrambling of the excess Et_3PAuSe-tagl according to eq 1a. It did not appear in Figure 5a−c. Two factors may contribute to its detection in Figure 5d, where Et_3PAuSe-tagl is in excess of the reduced cys-34 residue. First, the extent of disproportionation may be greater because the solvent for Figure 5d is more polar than that for Figure 5a (buffer vs 1:1 MeOD/buffer). Second, electrostatic binding of any of the equilibrium components of eq 1a to albumin can retard the rate of exchange, rendering it slow on the NMR time-scale and thereby allowing resolution of the individual components.

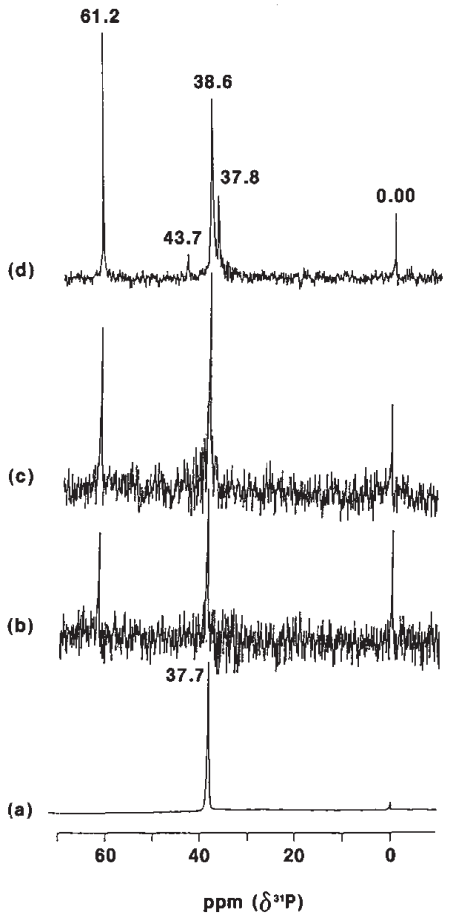

Figure 5. 31P{1H} NMR spectra of SeAF: (a) in methanol/buffer solution and (b−d) after incubation with BSA (4.1 mM, SH/BSA = 0.56), [Et3PAuSe-tagl]/AlbSH: (b) 0.25, (c) 0.48 (d) 0.89 in deuterated 100 mM NH_4HCO_3 buffer, pH = 7.9.

Because the extent of Et_3PO formation in Figure 5 exceeds that previously observed for reactions of BSA with Et_3P-AuCN[83] or Et_3PAuS-tagl,[11,14] a comparative study of reactions with Et_3PAuS-tagl, Et_3PAuCN, and Et_3PAuSe-tagl under identical, anaerobic conditions was carried out. ^{31}P NMR spectra were recorded within 1 h (Figure 6 a−c; left column) and at 24 h (Figure 6 a′−c′; right column) after mixing the reactants. The ratios of the Et_3PO (61.4 ppm) and $AlbSAuPEt_3$ (38.5 ppm) peak intensities, which reflect

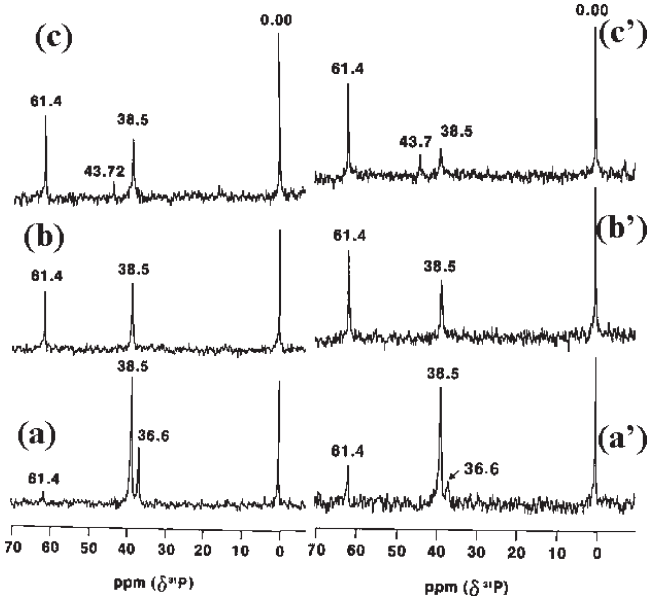

Figure 6. $^{31}P\{^{1}H\}$ NMR spectra of BSA (4.30 mM; SH/BSA = 0.56 in 100 mM deuterated NH_4HCO_3 buffer, pH = 7.9) incubated with Et_3PAuX (X = S-tagl, CN, Se-tagl; [Et_3PAuX]/[BSA] = 0.64) and measured within 1 h (a−c) and after 24 h (a′−c′); Et_3PAuS-tagl (a,a′), Et_3PAuCN (b,b′), and Et_3PAuSe-tagl (c,c′).

Scheme 2

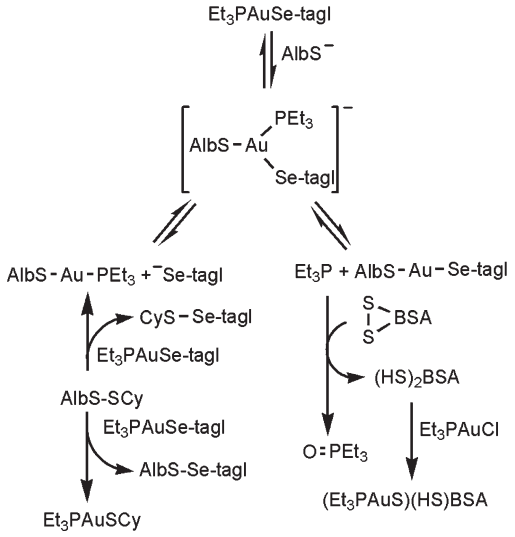

the extent of Et_3P oxidation, decrease in the following order:

$$Et_3PAuSe\text{-}tag1 > Et_3PAuCN >> Et_3PAuS\text{-}tagl$$

both at 1 h and after 24 h. No signals for Et_3PAuCN (35.4 ppm) or Et3PAuSe-tagl (37.8 ppm) were observed even at 1 h, although unreacted auranofin was still present after 24 h. For all three complexes, the Et_3PO concentrations increased over 24 h and the $AlbSAuPEt_3$ concentrations decreased, consistent with eqs 3a, 3b, and 4. The resonance of $[(Et_3P)_2Au]^+$ at 43.7 ppm appeared only for the Et_3PAuSe-tagl system. The albumin thiol titers, which measure the free sulfhydryl groups but not those coordinated to gold, were 0.18, 0.30, and 0.28 after reaction with Et_3PAuS-tagl, Et_3PAuCN, and Et_3PAuSe-tagl, respectively. The presence of sulfhydryl groups, in addition to the Cys-34 residues to which Et_3PAu^+ moieties are bound, is consistent with concomitant

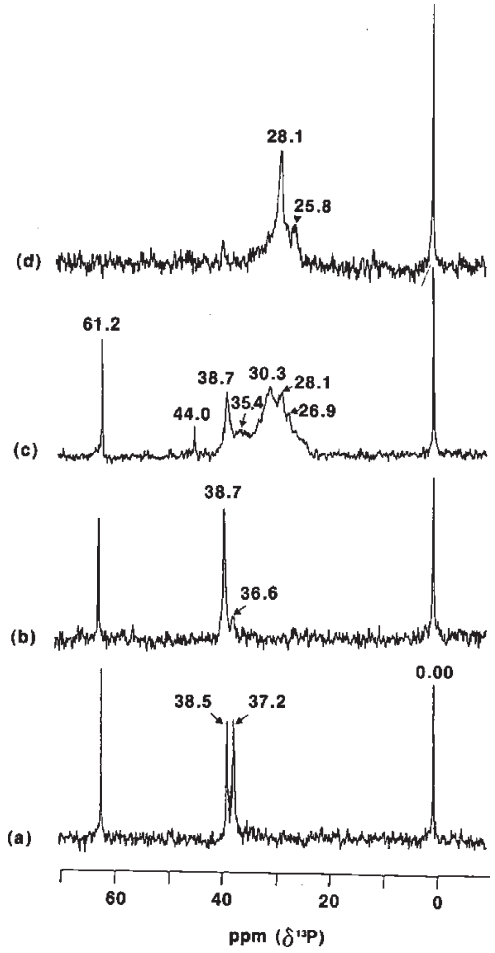

Figure 7. $^{31}P\{^{1}H\}$ NMR spectra in 100 mM deuterated NH_4HCO_3 buffer, pH = 7.9, of cysteine-blocked albumins: (a) 1.82 mM Ac-Cys +1.85 mM SeAF; (b) 4.05 mM Cys-BSA + 3.88 mM SeAF; (c) sample b + 8.04 mM Et_3PAuCl; (d) 3.81 mM Cy-BSA + 3.08 mM Et_3PAuCl.

reduction of internal disulfide bonds and oxidation of Et_3P (eq 4).

Sulfhydryl-modified albumins have been used previously to demonstrate that cysteine-34 is the principal gold binding site and to explore reactions at other sites on albumin.[10,14] Acetamide-blocked BSA (Ac-BSA) contains cysteine-34 that has been converted to a thioether, $AlbSCH_2CONH_2$, which is unable to displace phosphine, thiolate, or selenolate ligands from gold(I). Ac-BSA is a heterogeneous mixture consisting of ~60% $AlbS{-}CH_2CONH_2$ and ~40% naturally occurring disulfide-blocked albumins, principally AlbSSCy (where CySH = cysteine). Figure 7a shows the ^{31}P NMR spectrum obtained after the reaction between Et_3PAuSe-tagl and Ac-BSA. Resonances were observed for Et_3PO (61.2 ppm), $AlbSAuPEt_3$ (38.5 ppm), and Et_3PAuSe-tagl (37.2 ppm). Thus, unlike auranofin, Et_3PAuSe-tagl reacts with the disulfide bonds at Cys-34 of AlbSSCy to form $AlbSAuPEt_3$ and Et_3PO. Both the phosphine and selenolate ligands (eqs 5 and 6) can reduce the cysteine-34 disulfide to AlbSH:

$$AlbSSR + Et_3P + H_2O \rightarrow AlbSH + RSH + Et_3PO \quad (5)$$

$$AlbSSR + tagl\text{-}SeH \rightleftharpoons AlbSH + tagl\text{-}SeSR \quad (6)$$

The newly formed AlbSH reacts further with Et_3PAuSe-tagl to generate $AlbSAuPEt_3$, according to eq 2. After

chromatographic separation of the albumin from low-molecular weight species in the NMR sample, the albumin thiol titer was 0.65, and the Au_b/BSA ratio was 0.56. These values, given the initial mole ratio of ~0.40 AlbS−SCy present, reflect the fact that internal disulfide bonds as well as the cysteine-34 disulfide bonds are being reduced by Et_3P (eqs 3a, 4, 5) and/or tagl-SeH (analogous to reduction of AlbS−SCy via eq 6). The 35.8 ppm resonances previously observed for Et_3PAu^+ bound to sulfhydryl groups generated from internal disulfides are not observed, indicating the Et_3PAu^+ binds preferentially to Cys-34 or remains bound to the selenolate, consistent with their greater affinities for gold(I) compared to that of less acidic cysteine residues.[15,84]

To confirm that AlbSAuPEt$_3$ observed in Figure 7a was generated by reduction of the Cys-34 disulfide bonds, the reaction between Et_3PAuSe-tagl and Cys-BSA (100% disulfides at Cys-34, generated by reaction of BSA with cystine) was carried out at a 0.96:1.00 mol ratio. The ^{31}P NMR spectrum (Figure 7b) exhibited strong signals for Et_3PO (61.2 ppm) and AlbSAuPEt$_3$ (38.7 ppm) but not SeAF (37.8 ppm), indicating that it reacted completely. The weak resonance at 36.6 ppm is reasonably assigned to a small amount of $Et_3PAuSCy$ formed by free cysteine released from the Cys-34 disulfide bond according to eq 5, which is consistent with the SH titer of 0.79 measured after the reaction.

Reactions of Et_3PAuCl with the protein products present after obtaining spectrum 7b were carried out to confirm the presence of reduced thiols and to distinguish by NMR chemical shifts between the binding at Cys-34 (δ_P = 38.7 ppm) and the reduced internal disulfide sites (δ_P = 33−36 ppm). Two successive aliquots, each containing one equivalent of Et_3PAuCl, were added to the reaction mixture. After the first addition (not shown), the resonances at 38.7 and 36.6 ppm increased in intensity, indicating that additional reduced cysteine residues had been formed at cysteine-34 (AlbSH) and from internal disulfide bonds ($(HS)_2$Alb) by the initial reaction with Et_3PAuSe-tagl leading to spectrum 7b. Their respective Et_3PAu^+ adducts, identified by their characteristic chemical shifts, were formed by the added Et_3PAuCl as follows:

$$\text{Alb-S}^- + \text{Et}_3\text{PAuCl} \rightarrow \text{AlbSAuPEt}_3 + \text{Cl}^- \qquad (7a)$$

$$(\text{HS})_2\text{BSA} + x\text{Et}_3\text{PAuCl} \rightarrow (\text{Et}_3\text{PAuS})_x\text{BSA} + x\text{H}^+ + x\text{Cl}^- \qquad (7b)$$

The second Et_3PAuCl addition increased the Au_0/BSA ratio to nearly 3/1. The reduced SH groups became saturated, and the excess Et_3PAuCl reacted with some of the 17 histidine residues to form BSA−N_{His}AuPEt$_3$, accounting for the resonances between 30.3 and 25.3 ppm as shown in Figure 7c. AlbSAuPEt$_3$, $(Et_3PAuS)_x$BSA, BSA−N_{His}AuPEt$_3$ have been observed previously by ^{31}P NMR,[84,85] isolated, and characterized by EXAFS spectroscopy[10a,14] and more recently by ESI-MS studies of albumin reactions with Et_3PAuCl.[86]

Figure 7d demonstrates that the reaction between Cys-BSA and Et_3PAuCl in the absence of tagl-SeH, generates only the resonances at 28.1 and 25.8 ppm, characteristic of the histidine binding sites. No Et_3PAu-thiolate binding (33−38 ppm) is observed, because the oxidation−reduction processes of eqs 4−6 did not occur, demonstrating that Et_3PAuSe-tagl facilely generates new thiol sites ($(HS)_2$BSA and Alb-SH) in Cys-BSA and, therefore, can generate them from disulfides in native BSA, Ac-BSA, and perhaps in vivo from other proteins.

Table 2. Gold Binding to BSA and Cys-BSA

	$[Au]_0$/mM					
gold/protein ratios	1.61	3.31	4.55	5.88	7.14	8.33
Au_0/BSA[a]	0.39	0.78	1.17	1.55	1.93	2.32
Au_b/BSA[b]	0.32	0.45	0.61	0.72	0.75	0.75
Au_b/Cys-BSA[b]	0.34	0.48	0.61	0.78	0.85	0.88

[a] Initial ratios $[Et_3PAuSetagl]_0/[BSA]_0$ and $[Et_3PAuSetagl]_0/[Cys\text{-}BSA]_0$ used in the reaction mixtures. [b] Ratio of albumin-bound gold measured after chromatographic resolution of albumin-bound and free gold.

The extent of gold binding to BSA (containing mercaptalbumin) and to Cys-BSA (lacking mercaptalbumin) was compared by measuring protein-bound gold after chromatographic isolation of the protein from reaction mixtures with increasing concentrations of the seleno-auranofin. The data of Table 2 shows very little difference in the extent of gold bound (Au_b/BSA and Au_b/Cys-BSA) at low Au_0/BSA ratios (< 5) and slightly more bound to Cys-BSA at higher ratios (> 5). This reflects the ability of the seleno-auranofin to generate thiol binding sites in both forms of albumin and stands in contrast to earlier results with auranofin, in which reaction with Cys-BSA was negligible compared to BSA.[14]

Scheme 2 summarizes the reactions of AlbS$^-$ and AlbSS-Cy with Et_3PAuSe-tagl and the reduction of internal disulfide bonds to form $Et_3P{=}O$ and additional, weaker thiolate binding sites for gold. The oxidation of Et_3P is more rapid and extensive than previously observed for auranofin or Et_3PAuCN, suggesting that in vivo metabolism will proceed more rapidly, thereby quickly reducing the concentrations of Et_3PAuSe-tagl and the metabolites containing intact Et_3PAu^+ moieties.

Biological Activity. SeAF was tested in three different in vivo assays selected in order to determine its anti-inflammatory activity. For each assay, direct comparison with auranofin (AF) was made. The first protocol, the phorbol ester-induced inflammation (PEIF), utilizes the mouse ear to measure the inhibitory effects of drugs on the inflammatory response induced by phorbol ester.[50] This complex response utilizes edema or swelling mediated by cyclooxygenase−lipoxygenase products and inflammatory cytokines (e.g., IL-1 and TNF_α). The inhibition of swelling was determined by measuring ear thickness with a gauge after topical administration of a drug and compared to controls. Myeloperoxidase (MPO) activity was assayed as a measure of polymorphonuclear (PMN) leukocyte (white cell) infiltration. The data are displayed in Table 3. AF and SeAF showed comparable activity in the inhibition of ear swelling, whereas the PMN infiltration in this model and the next were less for SeAF than for AF.

The second protocol, the arachidonic acid (AA)-induced inflammation assay also involves the evaluation of a drug, topically administered, against mouse ear edema.[51] This test affords an advantage over the PEIF model in that it is sensitive to 5-lipoxygenase (5-LO) inhibitors but is relatively insensitive to selective inhibition of cyclooxygenase and affords a measure of a compound's anti-inflammatory activity.[51] The induced edema has a strong vasoactive amine component, but the MPO response appears to be 5-LO-product

Table 3. Phorbol Ester-Induced Inflammation

	% inhibition	
compound[a]	edema[b]	MPO[b]
AF	50***	59***
SeAF	57***	43**

[a] Dosed at 1 mg/ear; administered topically. [b] A double asterisk (**) denotes $p < 0.01$ and a triple asterisk (***) denotes $p < 0.001$ as significant differences from control with use of Student's t test. Results are based on eight mice per test group and eight mice in the control group, which were administered vehicle only.

Table 4. Arachidonic Acid-Induced Inflammation

		% inhibition	
	compound[a]	edema[d]	MPO[c]
A[b]	AF	0^{NS}	70***
	SeAF	0^{NS}	54**
B[c]	AF	11**	41***
	SeAF	12**	28**

[a] Dosed at 1 mg/ear; applied topically. [b] Experiment A: DMA vehicle. [c] Experiment B: 30 min pretreatment using acetone vehicle. [d] NS = not significant. A double asterisk (**) denotes $p < 0.01$ and a triple asterisk (***) denotes $p < 0.001$ as significant differences from control with use of Student's t test. Results are based on 5 mice per test group and 10 mice in the control group (administered vehicle only).

Table 5. Anti-inflammatory Activity of AF and SeAF in the Carrageenan-Induced Rat Paw Edema[a]

compound	oral dose mg Au/kg	% inhibition[b]	serum gold μg/mL[c]
AF	20	58***	1.66 ± 0.21
	10	28**	1.12 ± 0.09
	5	12^{NS}	0.88 ± 0.02
SeAF	20	12^{NS}	1.90 ± 0.20
	10	11^{NS}	1.06 ± 0.02
	5	9^{NS}	0.98 ± 0.05

[a] Three hour assay. [b] Percent of inhibition of paw volume increase in the rat carrageenan assay compared to controls. A double asterisk (**) denotes $p < 0.01$ and a triple asterisk (***) denotes $p < 0.001$ as significant differences from controls with use of Student's t test. Results are based on 6 rats per test group and 12 rats in the control group (administered vehicle only). [c] By GFAA, serum from control animals had 0 μg/mL of Au.

mediated. The data are shown in Table 4. Both AF and SeAF showed comparable activity in this assay although the anti-edema potency of both was considerably diminished compared to that observed in PEIF. Mechanistically, these results suggest that the gold compounds are not particularly good inhibitors of AA-induced edema, although inhibition of PMN infiltration remains high. This suggests that perhaps vasoactive amine response is not effectively inhibited. Again, AF appears to be more effective than SeAF.

Evaluation using the Carrageenan-induced rat paw edema assay constituted the third in vivo test of seleno-auranofin. This assay is a well-known model for inflammation employed to measure the effectiveness of various drugs as anti-inflammatory agents.[52] Auranofin, earlier, was reported to show good dose-dependent inhibition of rat paw swelling upon oral administration.[53] The data comparing AF with SeAF are reported in Table 5. Dose-dependent inhibition of paw edema by auranofin was also observed in this study at oral doses of 20, 10, and 5 mg per kg of gold. However, at the same gold-based doses, SeAF showed no significant activity. In light of the similar activity seen with AF and SeAF in the previous two topically administered studies, the lack of oral SeAF activity in the Carrageenan assay was surprising. Accounting for these observed differences remains speculative. SeAF may be more poorly absorbed across the gastrointestinal membrane of rats than AF, which itself is only 17−23% absorbed.[87] However, serum gold levels from AF- and SeAF-treated rats were similar (Table 5), suggesting comparable oral bioaccumulation of gold. Moreover, serum gold levels from AF-treated rats correlated with AF's effect on paw edema ($r = 0.77$; $p < 0.01$).

Alternatively ligand exchange reactions may occur in vivo differently with SeAF than with AF, thus preventing the gold from getting to the "active site". In the topical assays, ligand exchange leading to transport of gold is less of a problem because administration of the drug occurs directly at the site of activity. The exchange reactions of SeAF with serum albumin studied by ^{31}P NMR spectroscopy (above) demonstrate that formation of Et_3PO and reduction of protein disulfides to create new binding sites occur more rapidly and more extensively for Se-AF than for the comparable reactions of AF. Displacement of the triethylphosphine ligand from gold reduces the lipophilicity of the metabolites that form, which would in turn alter their tissue and cellular distribution patterns, consistent with the significantly reduced activity after oral administration.

Conclusions

Seleno-auranofin (Se-AF; Et_3PAuSe-tagl) was prepared in a two-step procedure derived from the synthesis of auranofin.[1] Extended X-ray absorption fine structure (EXAFS), X-ray absorption near-edge structure (XANES), and ^{197}Au Mössbauer spectra (Figures 1−3) confirmed a linear P−Au−Se coordination sphere in the solid state, analogous to the structure of auranofin.[59] ^{1}H and ^{13}C NMR parameters were generally similar to those of auranofin. The ^{31}P resonance at 35.11 ppm and the ^{77}Se resonance at 417.8 ppm in chloroform were singlets, consistent with rapid equilibration via ligand scrambling (eqs 1a and 2) to form $[Au(PEt_3)_2]^+$, $[Au(Se\text{-}tagl)_2]^-$, and $[(Et_3PAu)_2Se\text{-}tagl]^+$, which were identified in the Electrospray ionization mass spectrometry (ESI-MS) spectra (Figure 4). Binding to Cys-34, the only reduced cysteine in albumin, via displacement of the selenolate ligand is less extensive than the analogous reaction of AF, reflecting the greater affinity of selenolates vs thiolates for gold(I) (Figure 6). Yet, comparative ^{31}P NMR studies and measurement of protein-bound gold establish that Se-AF reacts more rapidly and more extensively than either Et_3PAuCN or Et_3PAuS-tagl with serum albumin to form Et_3PO, the metabolic product of the phosphine ligand in vivo (Figure 6, Table 2). Thus, the seleno-auranofin molecule, although selenolates have a higher affinity for gold(I) thiolates, is more rapidly degraded under biomimetic conditions.

Se-AF was comparable to AF in two topically administered tests of anti-inflammatory activity (phorbol ester- and arachidonic acid-induced inflammation assays in the mouse ear, Tables 3 and 4). Unlike AF, orally administered Se-AF was inactive in the Carrageenan-induced rat paw edema assay

(87) Intoccia, A. P.; Flanagan, T. L.; Walz, D. T.; Gutzait, L.; Swagzdis, J. E.; Flagiello, J.; Hwang, B.Y. H.; Dewey, R. H.; Nogochi, H. *J. Rheumatol.* **1982**, *9*(Suppl.8), 90–98.

(Table 5). The more rapid oxidation of triethylphosphine in the presence of serum albumin, resulting from a greater extent of ligand exchange reactions of SeAF, which in turn lead to less lipophilic metabolites, suggests that the in vivo metabolism and the transport of AF and SeAF will be significantly different. The reduced anti-inflammatory activity by oral administration, but not by direct, topical administration of Se-AF in comparison to AF, is consistent with the more rapid and extensive reaction of SeAF with albumin in vitro and may similarly be caused by more rapid metabolism in vivo.

Acknowledgment. The authors thank Gerald J. Capella for technical assistance in the preparation of this manuscript and Edie Reich for elemental analysis, both of GlaxoSmithKline Pharmaceuticals. A.A.I. thanks the Chemistry Department of the King Fahd University of Petroleum and Minerals, Dhahran, Saudi Arabia, for a sabbatical leave. C.F.S. acknowledges the support of Smith Kline Beecham, the NIH AR 39902, and the Illinois State University Department of Chemistry.

Abbreviations

Ad_2PzP = bis(adamantyl)benzylphosphine
AF = auranofin (Et_3PAuS-tagl)
$AlbS^-$ = mercaptalbumin component of serum albumin
AlbSSCy = cysteine-34 disulfide to another cysteine
$AlbSCH_2CONH_2$ = iodoacetate modified albumin
BSA = microheterogeneous albumin containing mercaptalbumin
Cys-BSA microheterogeneous albumin, primarily cysteine 34 disulfide form
Ac-BSA − microheterogenous albumin, contains $AlbSCH_2CONH_2$
*i*Bu = iso-butyl
Cy = cyclohexyl
Diap = 1,3-diazipane-2-thione
Diaz = 1,3-diazinane-2-thione
DiazSe = 1,3-diazinane-2-selenone
DMSO = dimethylsulfoxide
DTNB = 5,5′-dithiobis(2-nitrobenzoic acid)
ErgS = ergothionine
ESI-MS = electrospray ionization mass spectrometry
Et = ethyl
EtImSe = *N*-ethylimidazolidine-2-selenone
EtImt = *N*-ethylimidazolidine-2-thione
Et_2ImSe = *N*,*N*′-diethylimidazolidine-2-selenone
Et_2Imt = *N*,*N*′-diethylimidazolidine-2-thione
EXAFS = extended X-ray absorption fine structure
Ff = Fourier filtered
$(HS)_2AlbSX$ = any albumin molecule with a reduced internal disulfide bond
ImSe = imidazolidine-2-selenone
Imt = imidazolidine-2-thione
Me = methyl
MeImSe = *N*-methylimidazolidine-2-selenone
MeImt = *N*-methylimidazolidine-2-thione
mpt = 1-methyl-pyridine-2-thione
Ph = phenyl
PhImSe = *N*-phenylimidazolidine-2-selenone
PhImt = *N*-phenylimidazolidine-2-thione
Pr = propyl
*i*PrImSe = *N*-(*i*-propyl)imidazolidine-2-selenone
*i*PrImt = *N*-(*i*-propyl)imidazolidine-2-thione
*n*PrImt = *N*-(*n*-propyl)imidazolidine-2-thione
py = pyridine
SeAF = seleno-auranofin (Et_3PAuSe-tagl)
THT = tetrahydrothiophene (C_4H_8S)
TgS = thioglucose
TmS = thiomalate
p-tol = *para*-tolyl
XANES = X-ray absorption near-edge structure

Supporting Information Available: Supplemental Figures S1 and S2 show the calculated isotopic patterns for $[(Et_3PAu)_2(Se\text{-}tagl)]^+$ and $[Au(Se\text{-}tagl)_2]^-$. This material is available free of charge via the Internet at http://pubs.acs.org.